

Review

Dye-sensitized solar cells made from nanocrystalline TiO₂ films coated with outer layers of different oxide materials

K.M.P. Bandaranayake, M.K. Indika Senevirathna,
P.M.G.M. Prasad Weligamuwa, K. Tennakone*

Institute of Fundamental Studies, Hantana, Kandy, Sri Lanka

Received 15 October 2003; accepted 29 March 2004

Available online 25 May 2004

Contents

Abstract	1277
1. Introduction	1277
2. Experimental details	1278
3. Results and discussion	1279
3.1. Theoretical model 4.1	1280
4. Conclusion	1281
References	1281

Abstract

The material extensively used for construction of dye-sensitized solar cells is TiO₂. Similar cells made from other familiar semiconductor oxide materials such as SnO₂ and ZnO have yielded efficiencies far below the values corresponding to TiO₂-based cells. The indication is that electrons injected to s-band materials (SnO₂) are more susceptible to recombination compared to d-band materials (TiO₂). However, an impressive improvement in efficiency has been noticed when SnO₂ crystallites are coated with ~0.5–1 nm ultra-thin shells of high band gap oxides which act as a barrier against recombination. Naturally a barrier would also lower the electron injection efficiency and oxide barriers of thickness ~0.5–1 nm were noted to lower the efficiency of cells based on TiO₂. Contrary to our observation, reports in literature gives instances of obtaining higher efficiencies when TiO₂ crystallites in the film are coated with other oxide materials. In order to elucidate this problem an extensive series of experiments were conducted by coating TiO₂ crystallites with outer shells of different materials of varying thickness. Although there is some evidence for marginal improvement, efficiencies distinctively above the optimized TiO₂ could not be achieved by this technique. Experimental details and difficulties involved in making a clear conclusion are discussed.

© 2004 Elsevier B.V. All rights reserved.

Keywords: Dye-sensitization; Solar cells; Carrier recombination; Titanium dioxide; Tin oxide; Zinc oxide; Magnesium oxide

1. Introduction

Gratzel type dye-sensitized (DS) photoelectrochemical cells [1] (PECs) made from nanocrystalline TiO₂ films sensitized with ruthenium bipyridyl dyes are reported to have efficiencies ~10% [2]. Despite many attempts, an increase of efficiency above this optimum seems to be exceedingly difficult. Broadening of the spectral response and reduction of recombination losses are avenues available for improv-

ing the efficiency of the cell. Broadening of the spectral response requires synthesis of new dyes or devising ways of adopting dye mixtures for sensitization and this challenging issue has not been resolved. Although the incident photon to photocurrent conversion efficiency (IPCE) corresponding to the peak absorption position of the dye reaches values nearly unity, the short-circuit photocurrent (I_{sc}) at high intensities (one sun) in general does not commensurate with IPCEs measured at low intensities owing to trap filling and its effect on recombination. A more clearer sign of recombination is the deficiency of nearly 300 mV of the open-circuit voltage (V_{oc}) from the theoretical value.

* Corresponding author. Tel.: +94-8-232002; fax: +94-8-232131.

E-mail address: tenna@ifs.ac.lk (K. Tennakone).

Table 1

Photovoltaic parameters (I_{sc} : short-circuit photocurrent, V_{oc} : open-circuit voltage, η : efficiency, FF: fill factor) of DS cells made from SnO_2 , ZnO , TiO_2 , $[\text{SnO}_2]\text{MgO}$, $[\text{SnO}_2]\text{ZnO}$ and $[\text{SnO}_2]\text{Al}_2\text{O}_3$ films (illumination 1.5 AM, 1000 W m^{-2} simulated sunlight, cell area = 0.25 cm^2 , electrolyte composition: 0.6 M dimethyl propyl imidazolium iodide + 0.1 M LiI + 0.05 M I_2 + 0.5 M *t*-butyl pyridine in methoxyacetonitrile)

Cell	I_{sc} (mA cm^{-2})	V_{oc} (mV)	η (%)	FF (%)
SnO_2	12.0	330	1.3	32
ZnO	9.5	550	2.4	46
TiO_2	17.6	693	8.2	67
$[\text{SnO}_2]\text{MgO}$	15.1	725	7.1	65
$[\text{SnO}_2]\text{ZnO}$	16.9	665	6.5	58
$[\text{SnO}_2]\text{Al}_2\text{O}_3$	7.0	637	2.6	58

Efficiency (η), given in column 4, is the reproducible optimum obtained.

Recombination could occur via following paths: (1) geminate recombination of the injected electron with the dye cation D^+ ; (2) non-geminate D^+ , e^- recombination; (3) leakage of the electron to an acceptor in the electrolyte during transit through the nanocrystalline matrix (i.e., I_3^-).

The familiar high band-gap oxide semiconductors TiO_2 , SnO_2 and ZnO have similar band gaps and band positions and adsorbs N3 dye more or less to the same extent. Nevertheless when DS PECs are constructed from these materials (similar film thickness and morphology, same level of dye loading, same electrolyte) distinct differences are noted. TiO_2 cells yield the highest values of I_{sc} , V_{oc} , η and also the IPCE. SnO_2 happens to be the most inferior and ZnO gives slightly higher values for V_{oc} and η [3–5] (Table 1). Again we found that variation of crystallite size, film thickness and morphology, etc. did not enable the construction of DS PECs with ZnO or SnO_2 having efficiencies comparable to TiO_2 -based cells. As there is no evidence for large differences in the electron injection rates (ϕ_{in}) from excited dye molecules to these materials, we conclude that the inferior photovoltaic performance of DS SnO_2 and ZnO results from higher rates of recombination. If SnO_2 crystallites in a nanocrystalline film of SnO_2 are coated with an ultra-thin outer shell of MgO , ZnO or Al_2O_3 (we denote such films by the symbol $[\text{X}]\text{Y}$, where X and Y are core and

shell materials, respectively) and a DS PEC is constructed in the usual manner, the cell was found to have an efficiency comparable to the TiO_2 cell [4–6]. Undoubtedly, MgO acts as barrier greatly preventing recombination. In our earlier experiments [4,5], we did not observe an enhancement of the efficiency in depositing outer shell materials up to ~ 0.5 –1 nm on crystallites of TiO_2 films (i.e., $[\text{TiO}_2]\text{MgO}$, $[\text{TiO}_2]\text{Al}_2\text{O}_3$, $[\text{TiO}_2]\text{ZnO}$).

Contrary to our observations, the literature refers to instances where the results are suggestive of enhancement in efficiency obtained by coating outer shell materials on TiO_2 [7,8]. This paper describe some experiments we have conducted to determine whether the efficiency of TiO_2 -based DS PECs can be improved by forming outer shell structures of insulator or semiconductor materials (Fig. 1).

2. Experimental details

Nanocrystalline films of TiO_2 were deposited on conducting tin oxide (CTO) glass plates (0.5 cm \times 1 cm, sheet resistance = 12 Ωsq^{-1}) by the following procedure. 1 g of Degussa P25 TiO_2 powder was mixed into 30 ml ethanol containing 1 ml of acetic acid and five drops of Triton X-100 and the mixture was sonicated for 15 min and sprayed on to cleaned CTO glass plates placed on a hot plated heated to 150 $^\circ\text{C}$. The deposit was scraped off to leave a film of area 0.25 cm^2 and sintered at 450 $^\circ\text{C}$ for 30 min in air. Films of $[\text{TiO}_2]\text{MgO}$, $[\text{TiO}_2]\text{ZnO}$ and $[\text{TiO}_2]\text{Al}_2\text{O}_3$ were made by the same method after adding known quantities of Mg, Zn and Al acetates to the TiO_2 dispersion before sonication. The Mg, Zn and Al contents of the films were also confirmed by extraction of these metals from films into acidic medium and atomic absorption spectroscopic analysis. The following method was used to deposit outer shells of oxide materials conformally on TiO_2 crystallites. TiO_2 films are first deposited and the plates are heated in a solution (~ 0.01 M) of the respective acetate at 90 $^\circ\text{C}$ for ~ 20 min, rinsed with water and sintered at 450 $^\circ\text{C}$ for 10 min. Here, the hydrolysis of the acetate deposits the hydrous oxide of the metal (Mg, Zn or Al) on the TiO_2 surface and sintering converts it to the oxide. The surface coverage of the oxide is determined by extraction of the metal into strong HCl and atomic absorption spectrophotometric analysis. The median thickness of the TiO_2 films were estimated using a profilometer to scan the film surface and the film area determined by projecting the film to a screen. Films were made to adsorb the N3 dye by keeping them immersed in the dye solution for 10 h. Desorption of the dye from films of the same batch into an alkaline alcoholic solution enabled estimation of the surface coverage of the dye on the assumption that each dye molecule covers an area 1 nm^2 . Cells were formed by placing a platinum sputtered CTO glass plate in contact with the dyed surface and filling the capillary space between the plates with the electrolyte (0.6 M dimethyl propyl imidazolium iodide + 0.1 M LiI + 0.05 M I_2 + 0.5 M

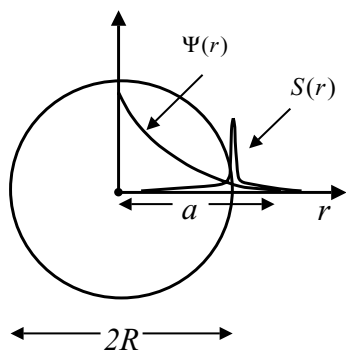


Fig. 1. A schematic diagram showing the wave functions $\psi(r)$ of an electron trapped at the center of a spherical particle (R = radius) and an electron in a surface state $S(r)$ at P. $S(r)$ is assumed to be a delta function.

t-butyl pyridine in methoxy-acetonitrile). *I*–*V* characteristics of the cells were recorded using a source meter and a intensity calibrated 1.5 AM, 1000 W m^{−2} solar simulator lamp.

3. Results and discussion

We estimate the thickness *T* of the shell material X in [C]X, with C as the core material using the formula

$$T = \frac{r}{3} \frac{W_X \rho_X}{W_C \rho_C} \quad (1)$$

where *r*: median radius of a core particle, *W_X*: weight of shell material, *W_C*: weight of TiO₂, *ρ_X*: density of the shell material. The thickness can also be related to the roughness factor *R* by the relation

$$T = \frac{W_C}{\rho_X R A}, \quad A = \text{film area} \quad (2)$$

Both Eqs. (1) and (2) assumes an uniform coverage of the shell material over the crystallites of the core material. Non-uniform distributions of X (especially the accumulation in the neck region) could have a profound influence on the cell performance. However, obtaining experimental evidence for such thickness variations would be very difficult. When X = MgO and C = TiO₂ the cell efficiency was reproducibly below that of pure TiO₂-based cells until X% in the film ~9% or greater (i.e., *T* computed from Eq. (1) is of the order of 0.05 nm or greater). On reducing the X% further we found that reproducibility of the results became more and more difficult and a large number of measurements were needed to make a decision of any statistical significance. Figs. 2–5 shows the variation of the short-circuit photocurrent (*I_{sc}*), open-circuit voltage (*V_{oc}*), and efficiency (*η*) and fill factor (FF). Clearly, all the above parameters except *V_{oc}* decrease with increase of MgO%. The same pattern of behavior was observed when we examined [TiO₂] ZnO and [TiO₂] Al₂O₃ films. At any surface coverage of ZnO or Al₂O₃, improvements in efficiency (above the pure TiO₂ cells) could not be achieved. Again when the procedure for conformal deposition of overlayers were adopted, we did not succeed in obtaining efficiencies above that of pure TiO₂-based cells. Overlayers on TiO₂, up to a point increases *V_{oc}* but *I_{sc}* and FF continuously decreases with the increase of X%. One difference we noted in the conformal method of deposition of films, was the tendency for the fill factor to increase initially, with increase of X%. Unfortunately, we could not obtain a statistically significant result indicative of a higher (i.e., above that of pure TiO₂-based cells) efficiency at the peak of FF.

The difference in the positions of the quasi-Fermi level (QFL) of the electrons in TiO₂ and redox-potential of the electrolyte determines the *V_{oc}* of the cell. The initial increase in *V_{oc}* with the MgO% (Fig. 3) indicates that the MgO overlayer acts as a barrier against recombination enabling the QFL to be raised. On further increase of the MgO%,

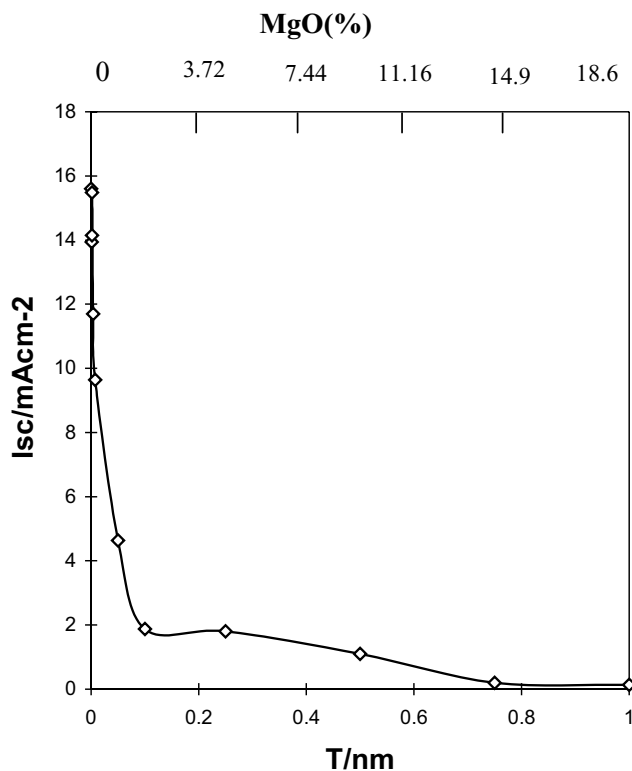


Fig. 2. Plot of the mean short-circuit photocurrent (*I_{sc}*) of [TiO₂]MgO cells vs. MgO% in the TiO₂ films and MgO shell thickness estimated from the Eq. (1).

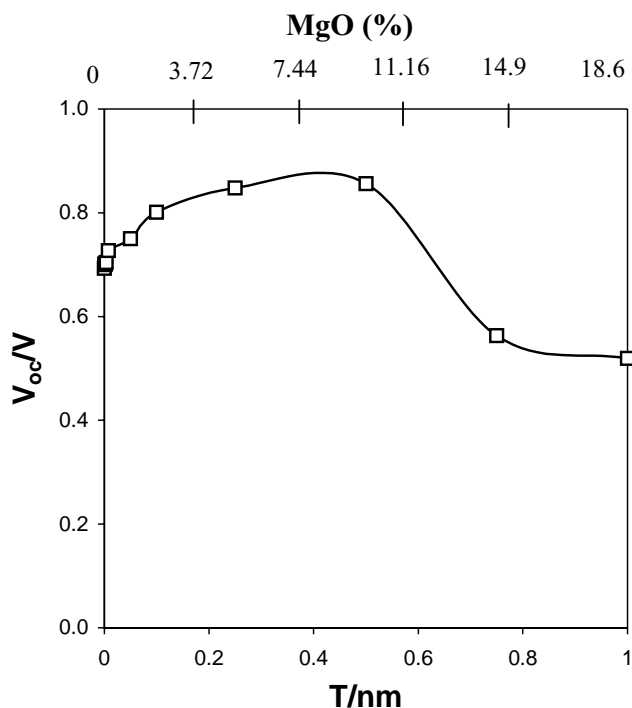


Fig. 3. Plot of the mean open-circuit voltage (*V_{oc}*) of [TiO₂]MgO cells vs. MgO% in the TiO₂ film and MgO shell thickness estimated from the Eq. (1).

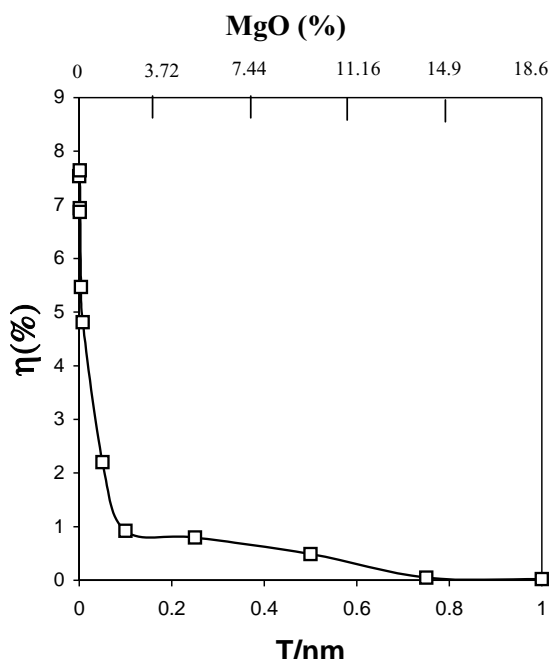


Fig. 4. Plot of the mean efficiency (η) of $[\text{TiO}_2]\text{MgO}$ cells vs. MgO% in the TiO_2 film and MgO shell thickness estimated from the Eq. (1).

the thicker barrier so rmed greatly reduces the electron injection efficiency from the excited dye molecules, lowering the QFL as the supply of electrons becomes limited and the V_{oc} begins to decrease once again. As expected this turning point of V_{oc} was found to depend on the intensity of light. We believe that the decrease in I_{sc} with MgO% is also a

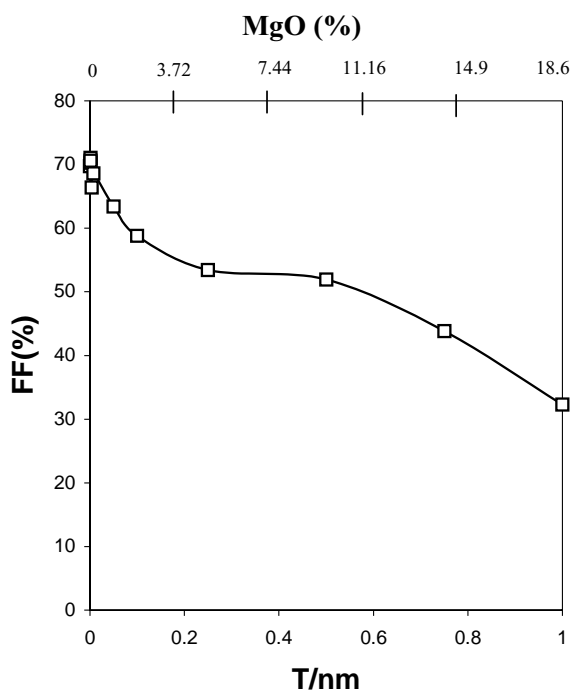


Fig. 5. Plot of the mean fill factor (FF) of $[\text{TiO}_2]\text{MgO}$ cells vs. MgO% in the TiO_2 film and MgO shell thickness estimated from the Eq. (1).

Table 2

Photovoltaic parameters (I_{sc} : short-circuit photocurrent, V_{oc} : open-circuit voltage, η : efficiency, FF: fill factor) of the cells made from TiO_2 and $[\text{TiO}_2]\text{MgO}$ films in an electrolyte (1.6 g tetra-propyl ammonium iodide + 0.12 g I_2 + 7.3 g ethylene carbonate + 2.7 ml acetonitrile) that excluded *t*-butyl pyridine (illumination 1.5 AM, 1000 W m^{-2} simulated sunlight, cell area = 0.25 cm^2)

Cell	I_{sc} (mA cm^{-2})	V_{oc} (mV)	η (%)	FF (%)
TiO_2	16.4	477	3.7	47
TiO_2/MgO	15.6	705	7.2	65

consequence of the lowering of the injection efficiency by the barrier. Contrary to the behavior of DS TiO_2 cells, DS cells made from nanocrystalline films of SnO_2 were found to improve greatly on coating the crystallites with overlayers of MgO, ZnO or Al_2O_3 . Here, the adverse effect of the barrier in reducing the injection rate greatly outweighs the gain resulting from the suppression of recombination. Yet, it is not easy to understand quantitatively how a $\sim 0.1 \text{ nm}$ MgO barrier on SnO_2 could increase the efficiency from 1.3 to 7.1%, whereas a barrier of the same thickness on TiO_2 decreases the efficiency from ~ 8 to 1%. The nature of the contact between the core and the shell (i.e., TiO_2/X compared to SnO_2/X) and their dielectric constants [9–11] could play an important role, but a consistent explanation is not possible at this stage. In all the above experiments the electrolyte contained *t*-butyl pyridine. We noticed an important difference when an electrolyte (1.6 g tetra-propyl ammonium iodide + 0.12 g I_2 + 7.3 g ethylene carbonate + 2.7 ml acetonitrile) that excluded *t*-butyl pyridine was used. Table 2 compares I_{sc} , V_{oc} , FF, η of cells made from TiO_2 and $[\text{TiO}_2]\text{MgO}$ (MgO $\sim 0.5\%$) films when the above electrolyte which excluded *t*-butyl pyridine is used. Clearly, in this situation V_{oc} and η are greatly enhanced in the $[\text{TiO}_2]\text{MgO}$ system. We noticed a similar effect in $[\text{TiO}_2]\text{ZnO}$ and $[\text{TiO}_2]\text{Al}_2\text{O}_3$ films. Overlayers of basic oxides at low surface concentrations seems to passivate recombination sites on the TiO_2 surface in the same way as *t*-butyl pyridine.

3.1. Theoretical model 4.1

The transition probability of an electron in a state ψ in the bulk of a semiconductor crystallite to a state S on the surface depends on the overlap integral (ψ, S) and if Σ is the surface density of trapping sites, the recombination rate Γ can be expressed in the form

$$\Gamma = A(\psi, S)^2 \Sigma \quad (3)$$

where A : constant. We have no direct experimental evidence to determine, whether state ψ would be a conduction band or a trap state. Electrons injected to a semiconductor will transit from conduction band to shallow traps from which they are re-emitted to the conduction band. If ψ is a conduction band state, we assume it takes the form

$$\psi_c = C \exp(ikr) \quad (4)$$

The wave function ψ_t of an electron in a shallow trap depth E below the conduction band has the form of a hydrogenic ground state given by

$$\psi_t = 2\alpha^{-3/2} \exp\left(\frac{-r}{\alpha}\right) \quad (5)$$

where

$$\alpha = \frac{\hbar}{(2m^*E)^{1/2}}$$

with m^* = effective electron mass. For the purpose of the model we assume that the surface state S is a delta function localized at the surface of the particle (Fig. 1), i.e.

$$S = \delta(r - R) \quad (6)$$

From the above equations the rates of recombination Γ_c and Γ_t via conduction band and trap states reduce to the expressions

$$\Gamma_c = BC^*C\Sigma, \quad B = \text{constant} \quad (7)$$

$$\Gamma_t = 4A\alpha^{-3} \exp\left(\frac{-2R}{\alpha}\right) \Sigma \quad (8)$$

As the probability current density (J) associated with the wave (3) is $\hbar k/m^*CC^*$, recombination via conduction band states becomes proportional to the current which the cell delivers, i.e., Γ_c can also be written in the form

$$\Gamma_c = \frac{Bm^*J\Sigma}{\hbar k} \quad (9)$$

The expression (7) tells us that trap mediated recombination would be appreciable only if $R \leq \alpha$. The parameter α (Bohr radius) depends on the effective electron mass and depth of the trap level below the conduction band edge. For thermally excitable traps $E \sim \kappa T$ (κ : Boltzmann constant, T : temperature) and α take the values 4.0 and 0.4 nm when $m^* = 0.1 m_e$ (SnO₂) and $10 m_e$ (TiO₂) respectively (semiconductors such as SnO₂ and ZnO where the conduction band is derived from s-orbitals have smaller effective mass compared d-band materials, i.e., TiO₂). Thus, trap mediated recombination would not be very high for TiO₂ films that generally have crystallite dimensions 10–50 nm. Whereas for SnO₂ films made from colloidal SnO₂ of median crystallite size ~ 3 nm trap mediation could be the major route of recombination. It is interesting to note that according to Eq. (9), recombination via conduction band states occurs at a rate proportional to m^* , suggesting that Γ_c may be higher for TiO₂ compared to SnO₂.

4. Conclusion

Experiments we have conducted did not give any evidence to conclude that the efficiency of DS cells based TiO₂ could be improved above an optimum of $\sim 8\%$ by coating overlayers of MgO, ZnO or Al₂O₃ by the methods

described in Section 2. When *t*-butyl pyridine is excluded from the electrolyte a light coverage of these oxides increased the efficiency well above that of similar cells made from bare TiO₂. The problem of comparing results of different experiments on DS solar seems to be the difficulty of quality control, especially the nanocrystalline film. Film crystallite sizes, thickness morphology are very sensitive to the slight deviations in the prescription used to fabricate the film. There are also variations in the contents of the electrolyte used by different workers and the moisture content of the electrolyte is not determined in most cases. As large standard deviations appear on statistical data analysis one could not readily arrive at conclusions regarding optimization of the system. We do not rule out the possibility of achieving higher efficiencies, on coating over layers by methods other than those presented in the experimental section. Although the efficiency of the optimized cell has not been exceeded, encouraging results have been obtained by conformal deposition of Al₂O₃ on TiO₂ [8].

Recombinations in DS solar cells could occur via conduction band or trap states. The theoretical analysis we have presented is not sufficiently refined to determine numerically the rate of each type of recombination. The rate of recombination depends on the availability of electron accepting surface states and factors that promote transition of electrons in the bulk of the crystallites to the surface states. Difference in behavior of DS solar cells made from nanocrystalline films of TiO₂ and SnO₂ and the explanations we have provided agree with the general consensus that traps contribute largely to recombination. The strategies available for mitigation of recombination are the removal of electron accepting surface states and/or ways of preventing leakage of electrons to these sites.

References

- [1] B.O. Regan, M. Gratzel, *Nature* 353 (1991) 737.
- [2] A.J. McEvoy, M. Gratzel, *Dye-Sensitized Regenerative Solar Cells*, in: S. Licht (Ed.), *Semiconductor Electrodes and Photoelectrochemistry*, Wiley-VCH, Weinheim, 2002, pp. 397–406.
- [3] K. Tennakone, G.R.R.A. Kumara, I.R.M. Kottegoda, V.P.S. Perera, *J. Chem. Soc. Chem. Commun.* 1999 (1999) 15.
- [4] K. Tennakone, J. Bandara, K.M.P. Bandaranayake, G.R.R.A. Kumara, A. Konno, *Jpn. J. Appl. Phys.* 40 (2001) L732.
- [5] G.R.R.A. Kumara, K. Tennakone, I.R.M. Kottegoda, P.K.M. Bandaranayake, A. Konno, M. Okuya, S. Kaneko, M. Murakami, *Semicond. Sci. Technol.* 18 (2003) 312.
- [6] A. Kay, M. Gratzel, *Chem. Mater.* 14 (2002) 2930.
- [7] A. Zaban, S.G. Chen, S. Chappel, B. Greg, *Chem. Commun.* 2000 (2000) 2231.
- [8] E. Palmares, N.J. Clifford, S.A. Haque, T. Lutz, J.R. Durrant, *J. Am. Chem. Soc.* 125 (2003) 475.
- [9] Y. Diamant, S.G. Chen, O. Melamed, A. Zaban, *J. Phys. Chem. B* 107 (2003) 1977.
- [10] S. Chappel, S.G. Chen, A. Zaban, *Langmuir* 18 (2002) 3336.
- [11] E. Palmares, N.J. Clifford, S.A. Haque, T. Lutz, J.R. Durrant, *Chem. Commun.* (2002) 1464.